Research article

Four-scroll attractor on the dynamics of a novel Hopfield neural network based on bi-neurons without bias current

Bertrand Frederick Boui A Boya [a,b,*], Jacques Kengne [a], Germaine Djuidje Kenmoe [b], Joseph Yves Effa [c]

[a] Research Unit of Automation and Applied Computer (UR-AIA), Electrical Engineering Department of IUT-FV, University of Dschang, P.O. Box 134, Bandjoun, Cameroon
[b] Laboratory of Mechanics, Department of Physics, Faculty of Science, University of Yaoundé 1, Yaoundé, Cameroon
[c] Department of Physics, University of Ngaoundere, P.O. Box 454, Ngaoundere, Cameroon

ARTICLE INFO

ABSTRACT

The dynamics of a neural network under several factors (bias current and electromagnetic induction effect) are recently used to simulate activities of the brain under different excitation. In this paper, we introduce a novel Hopfield neural network (HNN) based on two neurons with a memristive synaptic weight connected between neuron one and two based of flux controlled memristor recently proposed by Hua M. et al., in 2022. Using analysis tools, we proved that this model can develop rich dynamical characteristics such as various number of equilibrium points when the parameters are varied, four-scroll attractors, transient chaos, multistability of more than three different attractors and intermittency chaos phenomenon are reported. Moreover, when increasing a synaptic weight, the model shows bursting oscillations phenomenon. To obtain the normal state of the brain, the control of multistability to a strange monostable state is carry out. Finally, microcontroller implementation of the model is considered to verify the numerical analysis.

1. Introduction

The human brain is a complex biological nervous network composed of a great number of interactive neurons. Artificial neural networks are proposed for the purpose of imitating human brain function. Based on the brain nervous topology, a simplified brain neural network was constructed by Hopfield in 1982 [1]. Recently Hopfield neural network have been investigated with different topology who is able to generate complex phenomena with a simplest configuration chaos [2, 3, 4], hyperchaos [5, 6], multi-scroll [7, 8], antimonotonicity [9] and bursting oscillation [10] to name a few. Memristive synapse can be used to emulate the electromagnetic induction effects. Electromagnetic radiation has an effect on the functional behavior of the brain system, and appropriate electromagnetic radiation. W. Fuqiang et al., recently reproduce the biophysical function of chemical synapse by using a memristive synapse and helps to stimulate neurons to produce multiple patterns of electrical activity [11]. Han B. et al., proposed a 5D neuron model of two adjacent neurons coupled by memristive electromagnetic induction

and exhibits complex multiple firing patterns [12]. Ref [13] develop the effects of electromagnetic radiation distribution on the neural network based on n neurons. Where the dynamic behaviors develop chaos, transient chaos and hyperchaos. An improved neuron model is proposed to explore the effect of the magnetic field from the physical aspect. By connecting a memristor with Hodgkin-Huxley neuron model literature [14] proved that the neuron under stimuli is close to the intrinsic frequency of the neuron, and then bursting. Li H. et al., [15] develop a three dimensional HNN with different types of external stimuli. This configuration can produce complex multi-scroll attractors. Especially, some researchers discovered that more complicated chaotic attractors can be engendered in some memristive Hopfield neural networks through introducing a memristor as a neural synapse with simplest configuration. The dynamic behaviors of HNN associated with the self-coupling strength of the memristive synapse are investigated in ref. [16] and revealed complex dynamic such as bursting oscillation and multistability within bias current. A two-neuron-based non-autonomous Hopfield neural network (HNN) with external stimulus is presented in [17],

---

* Corresponding author at: Research Unit of Automation and Applied Computer (UR-AIA), Electrical Engineering Department of IUT-FV, University of Dschang, P.O. Box 134, Bandjoun, Cameroon.
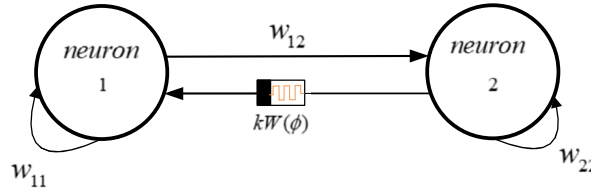*E-mail address:* bertrandboui22@yahoo.com (B.F.B.A. Boya).

Fig. 1. Topological connection of HNN based of bi-neurons with single memristive synaptic weight.

within the stimulus-associated dynamical behaviors includes limit cycles, chaotic attractors, period-doubling bifurcation and bistability are revealed. A new two-neuron-based non-autonomous memristor-based Hopfield neural network employing a memristor as a self-connection synapse is presented in literature [18], were the shown transient chaos and various coexistence of four different attractors within bias current. C. Chen et al., proposed a non-ideal memristor synapse is employed to emulate an electromagnetic induction current caused by the potential difference between two neurons with the coexisting chaotic and two stable point attractors [19] without bias current. Furthermore, M. Hua et al., [20] present a memristive single neuron model where the found interesting phenomena such as double-scroll attractors, coexistence of three periodic attractors, and some bursting firing patterns are shown. NIST test prove that four scroll attractor has better randomness and robustness than the two-spiral attractors, which means that the high quality random sequences generated by the four-scroll attractor is more conducive to image encryption [8]. According to this idea, Yu F. et al., present a dynamical behaviors of multi-scroll attractor based on fractional order memristive Hopfield neural network model, and used the plethora behaviors for audio encryption scheme [21].

Inspired by the above works, we proposed a simple neural network with more complex dynamic when the model present two neurons and we highlight the rich repertoire of behaviors such as four-scroll chaotic attractor, multistability, various busting oscillation, intermittency and transient chaos phenomenon. Moreover, control of four different periodic state of the brain behaviors by using linear augmentation method to cure the pathological state of the brain. Microcontroller based implementation is carried out for experimental investigation.

The rest of this work is organized in the following way. Section 2 present the novel model, the analysis of the equilibrium points with its corresponding stability is studding. The numerical study, is conducted in section 3 to show the complex dynamic behaviors of the model. Moreover, control of multistability is considered in section 4. Experimental investigation are present in section 5. Finally, the last section concludes the paper.

2. Theoretical study

The new HNN with memristive synaptic weight considered in this work is obtained from the well-known Hopfield model equation (1a) with activation function described in equation (1b). We connect a memristor between neuron 1 and 2 as shown in Fig. 1 with memristor equation (2) recently introduced in literature by M. Hua et al., in 2022. The resulting of mathematical model is shown in equation (3). Where w_{11}, w_{12}, and w_{22} represent the synaptic weight of the neurons. k is the coupling string between neuron 1 and 2.

$$\begin{cases} \dot{x}_1 = -x_1 + w_{11}f_1(x_1) + w_{12}f_2(x_2) \\ \dot{x}_2 = -x_2 + w_{21}f_1(x_1) + w_{22}f_2(x_2) \end{cases} \tag{1a}$$

$$f_i(x_i) = \tanh(2x_i - 3) + \tanh(2x_i + 3) - 2\tanh(2x_i) \tag{1b}$$

$$\begin{cases} I_M = kW(\phi)V_M = k(\phi^2 - 0.5)V_M \\ \dot{\phi} = V_M - 2\phi \end{cases} \tag{2}$$

$$\begin{cases} \dot{x}_1 = -x_1 + w_{11}f_1(x_1) + w_{12}f_2(x_2) \\ \dot{x}_2 = -x_2 + k(\phi^2 - 0.5)f_1(x_1) + w_{22}f_2(x_2) \\ \dot{\phi} = f_1(x_1) - 2\phi \end{cases} \tag{3}$$

Table 1. Equilibrium points, eigen values and stability of the system for discrete value of k and others parameters setting $w_{11} = -0.97$, $w_{12} = 1.25$, $w_{22} = 0.2$.

	Equilibrium points $P_{0,1,2}$	Eigen values $\lambda_{1,2,3}$	Stability
$k = 0.2$	$P_0 = (0,0,0,0)$	$3.200 + 0.000i$ $-2.075 \pm 1.935i$	Unstable
	$P_{1,2} = (\pm 1.532, \mp 0.066, \mp 0.463)$	$-4.901 + 0.000i$ $-0.887 \pm 2.115i$	Stable
	Equilibrium points $P_{0,1,2,3,4}$	**Eigen values $\lambda_{1,2,3}$**	**Stability**
$k = 1$	$P_0 = (0,0,0)$	$1.552 + 0.000i$ $-1.251 \pm 2.220i$	Unstable
	$P_{1,2} = (\pm 0.213, \mp 0.104, \mp 0.397)$	$1.843 + 0.000i$ $-1.700 \pm 1.994i$	Unstable
	$P_{3,4} = (\pm 1.404, \mp 1.035, \mp 0.587)$	$-2.585 \pm 0.855i$ $-0.505 + 0.000i$	Stable

2.1. Dissipation property

It is known that nonlinear dissipative systems can experience chaotic attractors [22]. To have an idea of the type of dynamics the considered model is able to generate, its volume contraction rate obtain the contraction rate as:

$$\nabla V = -4 + w_{11}g_1 + w_{22}g_2 \tag{4a}$$

$$g_i = 2\tanh^2(2x_i - 3) + 2\tanh^2(2x_i + 3) - 4\tanh^2(2x_i) \tag{4b}$$

Since $-1 \le g_i \le 1$, for the a good choice of w_{11} and w_{22}, the model can be dissipative according to equation (4a)–(4b). Then, the existence of an attractor is proven in the memristive Hopfield neural network model.

2.2. Equilibrium points and their stability

As for the model given in equation (3), the equilibrium points is obtained as $P_n = \left(x_{1e}^n, x_{2e}^n, 0.5f_1(x_{1e}^n)\right)$ which is graphically solved using with transcendental equation (5). n is the numbering index of equilibrium points x_{1e}^n, which corresponds to the graphical intersections with the abscissa of the solution curve in equation (5). For some value of the parameter k we present the curve equation (5) in Fig. 2(a)-(b) wish shown three and nine intersections with the X-axis, for some critical values $w_{11} = -0.97$, $w_{12} = 1.25$, $w_{22} = 0.2$. The number of the intersection of solution curve with the X-axis coincides with the number of the equilibrium point.

$$S(x_{1e}) = -x_{1e} + w_{11}f_1(x_{1e}) + w_{12}f_2(x_{2e}) \tag{5}$$

The Jacobean matrix of system equation (3) is described in equation (6). Characteristic equation associated with to this model is obtained from the MATLAB software and the eigen values show issues of the stability of the model according to the equilibrium points. The stability of the model is summary in Table 1, where we remark that the model present stable and unstable state for some value of the coupling string. The presence of Hopf bifurcation are emerged in this model.

$$J = \begin{bmatrix} -w_{11}g_1 - 1 & -w_{12}g_2 & 0 \\ -k(\phi^2 - 1/2)g_1 & -w_{22}g_2 - 1 & 2k\phi f_1(x_1) \\ -g_1 & 0 & -2 \end{bmatrix} \tag{6}$$
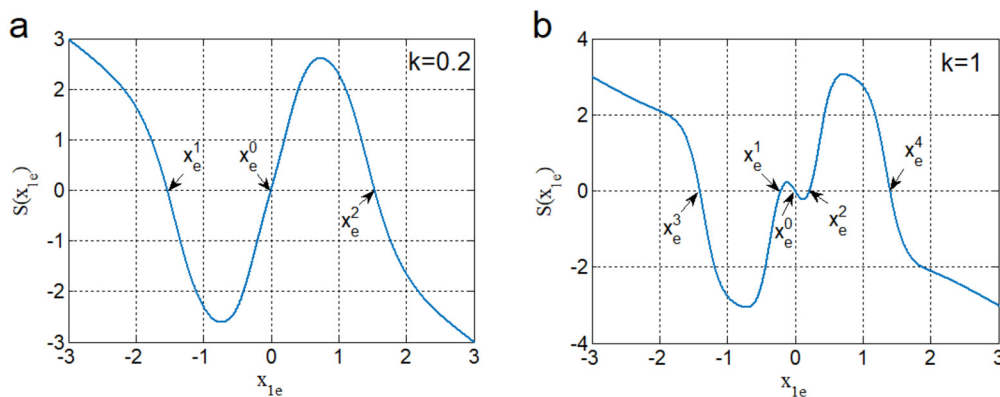
Fig. 2. Intersection points of function curve given by equation (5) showing the effect of coupling strength on the equilibrium points when parameters are fixed $w_{11} = -0.97$, $w_{12} = 1.25$, $w_{22} = 0.2$.
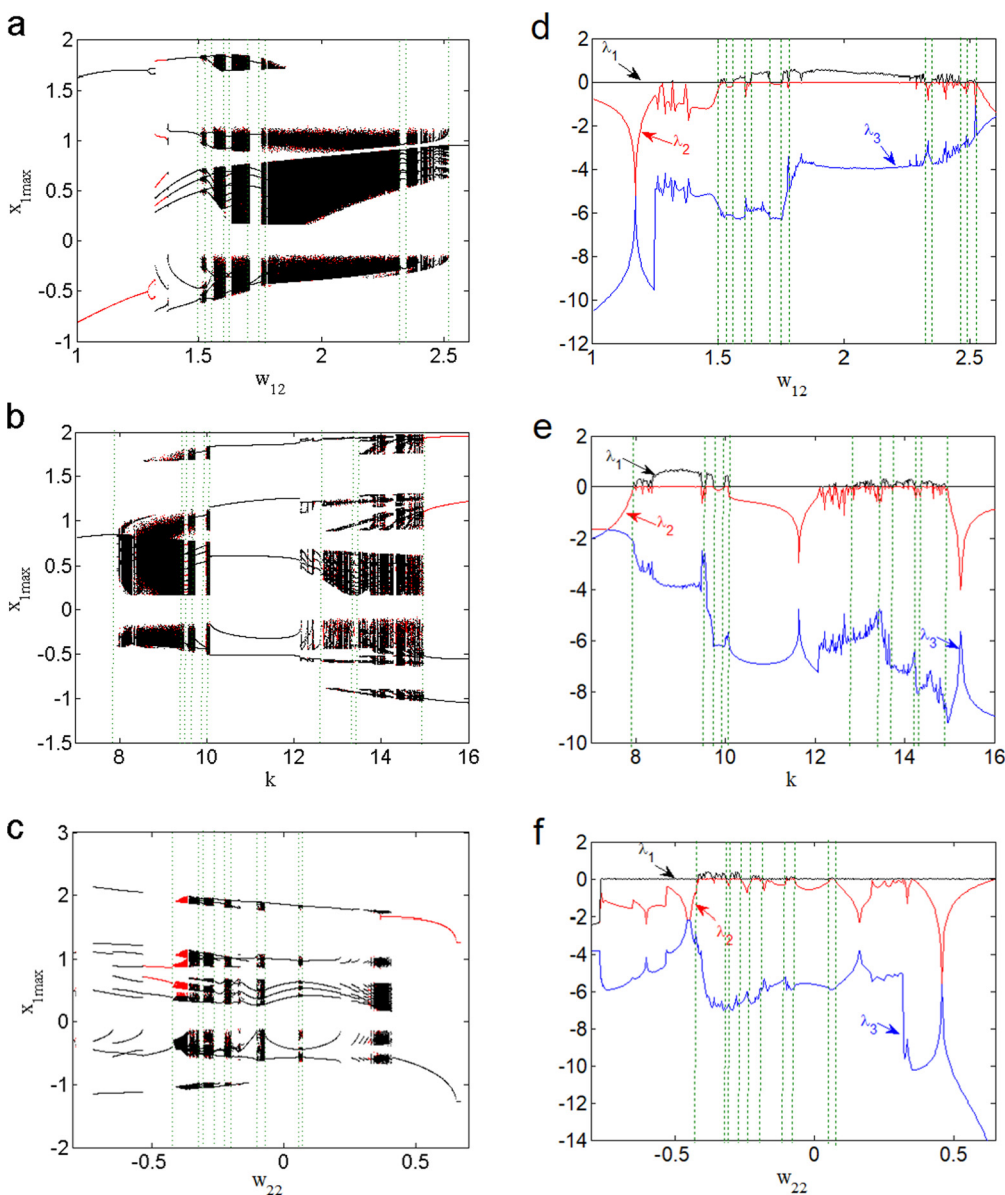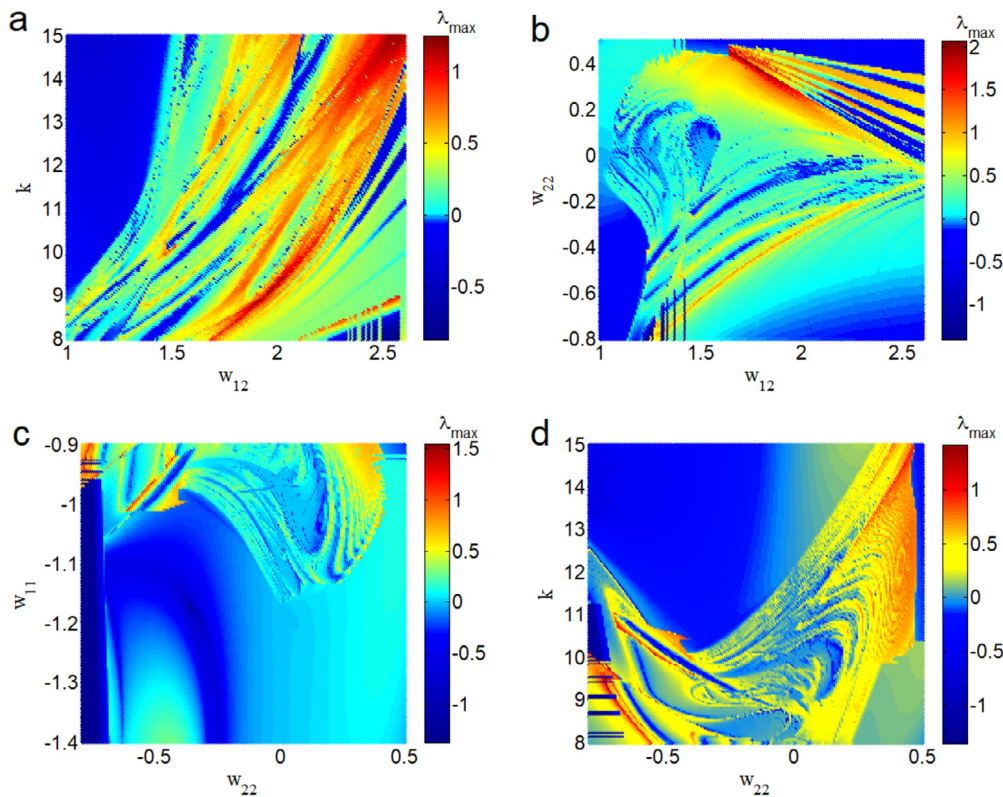

Fig. 3. (a-b-c) Bifurcation diagram displaying local maxima of x_1 when we increase synaptic weights and coupling strength. With corresponding (c-d-f) plot of Lyapunov spectrum scanned upward from initial conditions $(\pm 1, 0, 0)$ with chaotic area delimited in green boundary points.

Fig. 4. Two parameter Lyapunov diagrams in different planes. (a) Plane (w_{12}, k); (b) plane (w_{12}, w_{22}); (c) plane (w_{22}, w_{11}); (d) plane (w_{22}, k) with initial conditions $(1, 0, 0)$.

3. Numerical investigation

To address this subsection, numerical simulations will be done on the system (3) by means of the Runge–Kutta algorithm with time step $\Delta = 0.005$ and $t \in [5000, 10000]$ for a good precision and to remove the transient state on the model. Fig. 3 provides three different intermittence bifurcation diagrams of parameter w_{12}, k and w_{22} (see Fig. 3 (a)-(b)-(c) respectively) of the model (3) and their corresponding Lyapunov spectrum in Fig. 3 (d)-(e)-(f). Draw in upward direction with initial conditions $(\pm 1, 0, 0)$ and parameter set as $w_{11} = -1.1$, $w_{12} \in [1, 2.6]$, $k = 10$, and $w_{22} = 0.3$ for Fig. 3 (a); $w_{11} = -1.1$, $w_{12} = 1.7$, $k \in [7, 16]$, and $w_{22} = 0.3$ for Fig. 3 (b); and $w_{11} = -0.97$, $w_{12} = 1.25$, $k = 10$, and $w_{22} \in [-0.8, 0.57]$ for Fig. 3 (c). The above bifurcation diagrams of system (3) are symmetrical and present some hysteresis dynamics with chaotic area delimited in green boundary points.. The variation of two parameters of the model are computed to characterize the global dynamics of the model. Fig. 4 is obtained when two different sets of parameters are varied among them; (w_{12}, k) (see Fig. 4 (a)), (w_{12}, w_{22}) (Fig. 4 (b)), (w_{22}, w_{11}) (see Fig. 4 (c)), and plane (w_{22}, k) (Fig. 4 (d)). From this figure, the model under consideration is able to exhibit complex activity depending on the sign of the largest Lyapunov exponent. When $\lambda_{\max} < 0$ the model present rising activities. Periodic activities are characterized by $\lambda_{\max} = 0$, and chaotic activities are characterized by $\lambda_{\max} > 0$. Therefore, it is obvious to conclude this model is able to exhibit the complex of four-scroll strange attractors as present in Fig. 5. When the increase the value of synaptic weight w_{22} such as $w_{22} = -0.3648$, $w_{22} = -0.32$, $w_{22} = -0.073$, and $w_{22} = 0.387$ (see Fig. 5 (a1-c1) respectively). Projection in (x_1, x_2) and the strange attractors in space (x_1, ϕ, x_2) (Fig. 5 (a2-c2)) for initial conditions $(0, 0, 0)$.

3.1. Multistability

Multistability of different attractors for a given set of parameters is one of the fundamental properties of nonlinear dynamical systems [23]. Coexistence of multiple attractors have a great importance in the brain dynamics, which exhibits multistable coordination dynamics at many levels, from multifunctional neural circuits in vertebrates and invertebrates to large-scale neural circuits in humans [24, 25, 26]. Multistability in neuronal networks can mark either a normal (chaotic) or a pathological state (periodic) of brain [27, 28]. We have exhibited through the Fig. 3 (c), the coexistence of various attractors as illustrates in Fig. 6. Coexistence of two limit cycles period- 4 with fixed point for $w_{22} = -0.7872$ (see Fig. 6 (a)), bistability of double chaotic scroll attractors when $w_{22} = -0.376$ present in Fig. 6 (b). Coexistence of four different attractors such as symmetric limit cycle period-2 and 4 for $w_{22} = -0.381$ as shown in Fig. 6 (c1)-(c2). Coexisting of symmetric limit cycle period-1 with fixed point and one strange attractors of four-scroll is provided in Fig. 6 (d1)-(d2) for $w_{22} = 0.3867$. Poincare section supplied regular and irregular open curves (see Fig. 7(a)-(b)), which justified coexistence of different attractors observed from this model. It is interesting to see that the model can present complex phenomenon of various coexistence.

3.2. Intermittency and transient chaos

Transient chaos is a situation where to a situation where trajectories starting from randomly chosen initial conditions of chaos and then, suddenly switches over into a final non chaotic dynamic [29]. Intermittency is the presence of more than two different state (chaotic and nonchaotic) according to the same initial condition [30]. This phenomenon can be regarded as a type of multi-stable state [29]. For the system (3), the numerical analysis showed transient chaos according to
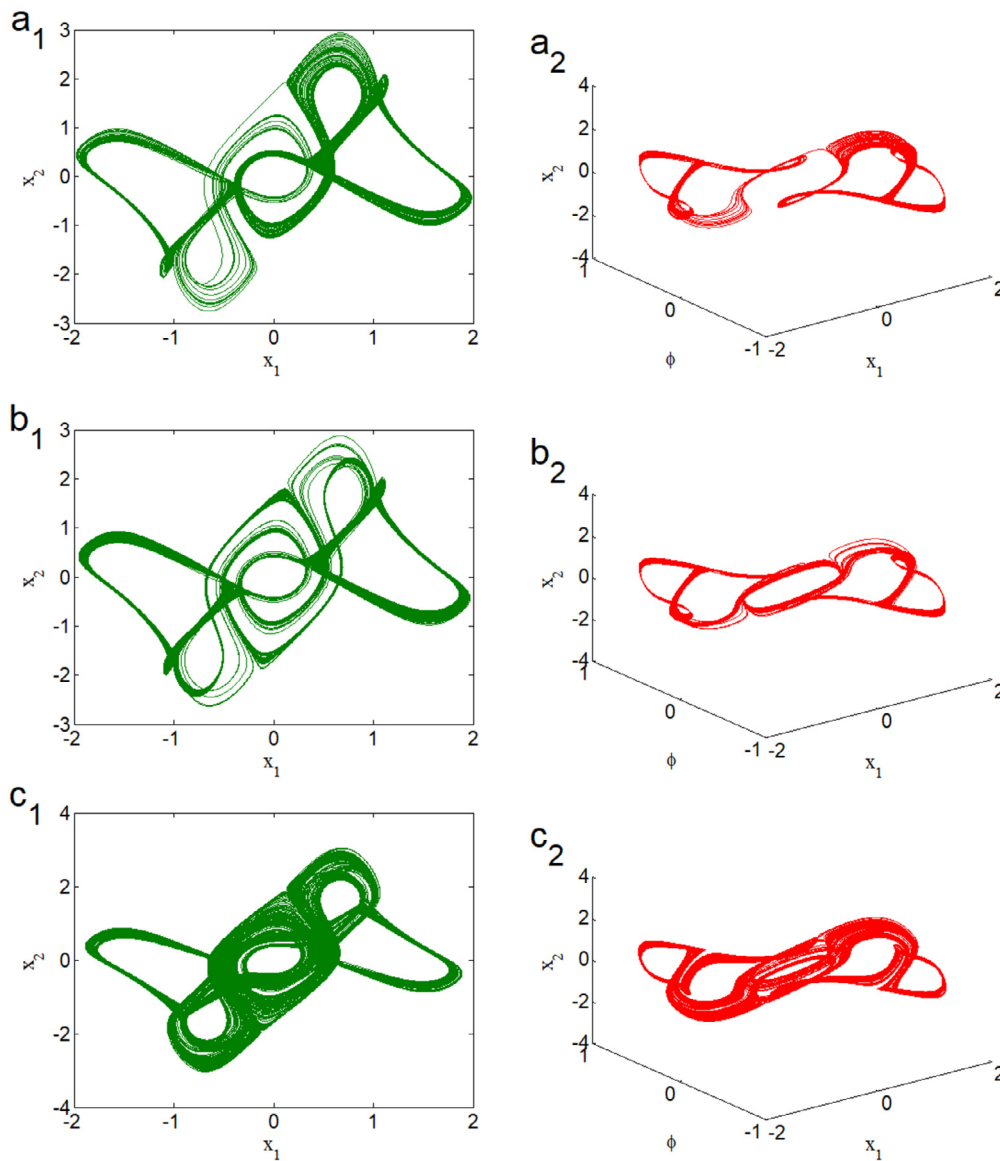
Fig. 5. Phase portraits displaying four-scroll attractors plot in the plane (x_1, x_2) and space (x_1, ϕ, x_2). (a) $w_{22} = -0.3648$, (b), $w_{22} = -0.32$, and (c) $w_{22} = -0.073$, for initial conditions $(0, 0, 0)$.

Fig. 3 (c), using time series and phase portrait as shown in Fig. 8 (a)-(b) respectively. Where we present four-scroll attractor in green and limit cycle periodic-7 in black color for $w_{22} = -0.0712$ and initial conditions $(0, 1, 2.1)$. Wherever, the intermittency chaos, is reveled in this model. Fig. 9 (a)-(b) present respectively on time series and phase portrait the evolution of this phenomenon within this system. Strange attractor is shown in green color, two different limit cycle periodic-10 and 7 red and black color is present respectively for $w_{22} = 0.387$ and initial conditions $(0, 1, 0.1)$.

3.3. Bursting oscillation

Bursting oscillation, as a very complex nonlinear phenomenon of alternations between fast states and slow states, is often applied for communication in biological neurons [10, 31]. By increasing the values of synaptic weight w_{22} and set parameter as $w_{11} = -1.1$, $w_{12} = 1.7$, and $k = 14.8$. We proved presence of regular and irregular symmetric bursting oscillation. Fig. 10 displaying time series and phase portrait of the evolution of this phenomenon. For $w_{22} = 0.278$, and $w_{22} = 0.29$ the model present regular bursting as provided Fig. 10 (a1)-(a2)-(c1)-(c2).

When $w_{22} = 0.285$, the system involved irregular bursting oscillation (see Fig. 10 (b1)-(b2)) with initial conditions $(\pm 1, 0, 0)$.

4. Control of multistability

Multistability plays a great flexibility in the performance of dynamical system. Wherever, periodic orbit are not desirable in neural system (coexistence of normal and pathological states in the brain). Hence, the necessity to design a control will enable us to move periodic states and maintain the chaotic state. Recently, By using the temporal feedback method introduced in [32], Z. Njitacke and collaborators explored it to control any desired state without any modification of the topological structure of the attractors associated with that state. Wherever, this method is limited when the model present only coexistence of periodic state. To the aims of this issues, we perform the linear increase control present in [33, 34] to resolve the problem of periodic state in brain. Here, we explore a control of multistability using linear increase (equation (7)) for multistability of four different periodic attractors ($w_{22} = -0.381$).
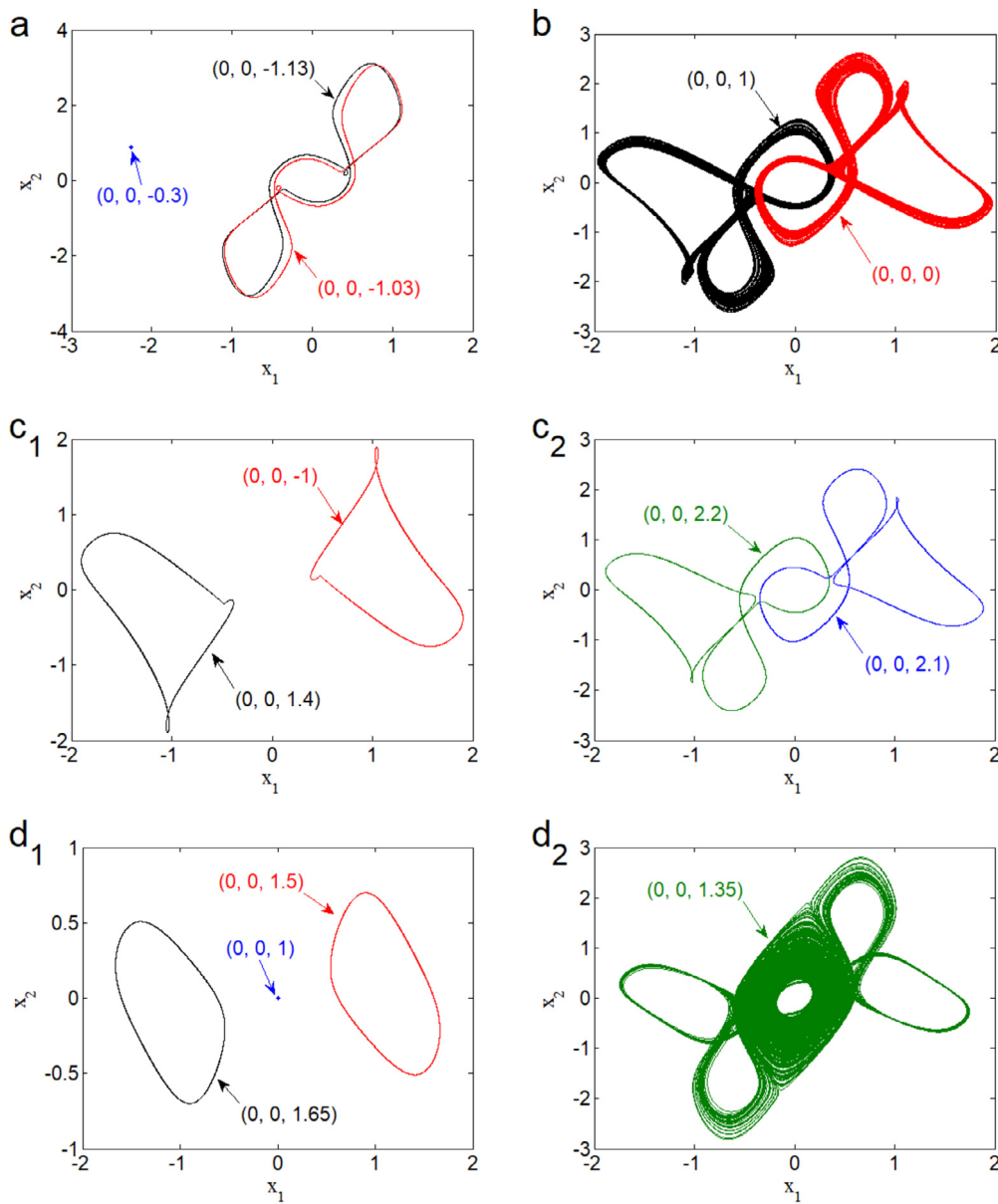
Fig. 6. Phase portraits illustrating coexistence of multiple attractors plot in the plane (x_1, x_2). (a) $w_{22} = -0.7872$ coexisting symmetric limit cycle period- 4 with fixed point; (b) $w_{22} = -0.376$ coexisting symmetric two-scroll chaotic attractors; (c) $w_{22} = -0.381$ coexisting symmetric limit cycle period-2 and 4; (d) $w_{22} = 0.3867$ coexisting symmetric limit cycle period-1 with fixed point and four-scroll attractor.
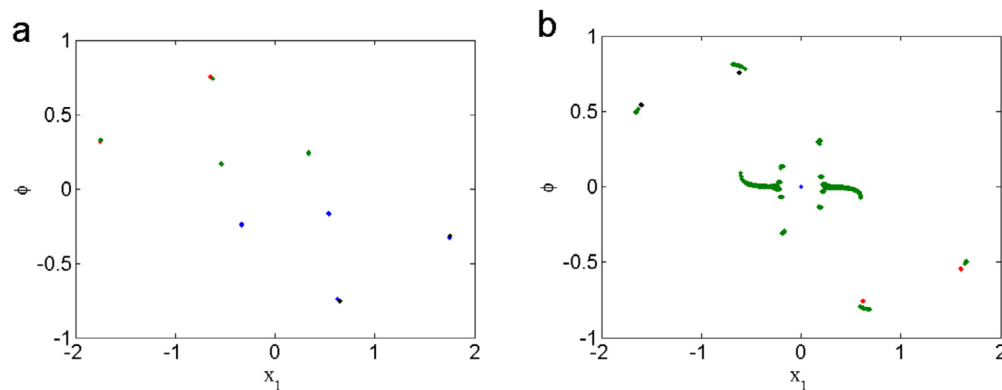
Fig. 7. (a)-(b) Poincare mapping of coexistence of four different attractors as in Fig. 6 (c)-(d) respectively with the corresponding color of attractors.
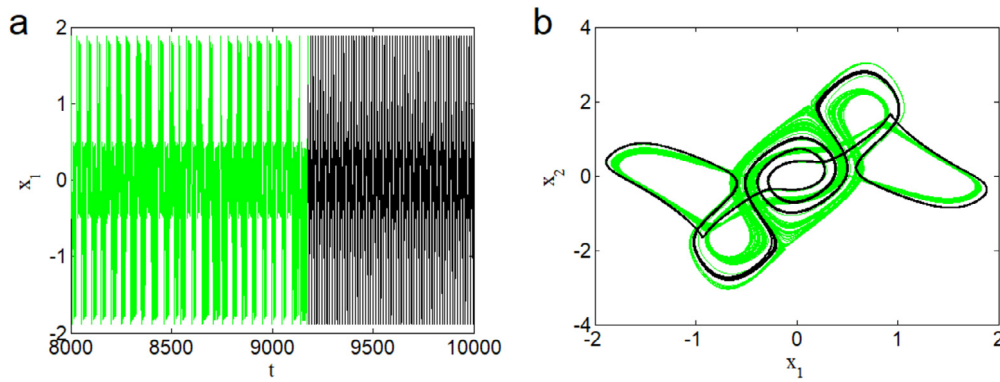
Fig. 8. Time series and phase portrait showing the transient chaos (four-scroll attractor in green and limit cycle periodic-7 in black color) observed in this model for $w_{22} = -0.0712$ and initial conditions $(0, 1, 2.1)$.
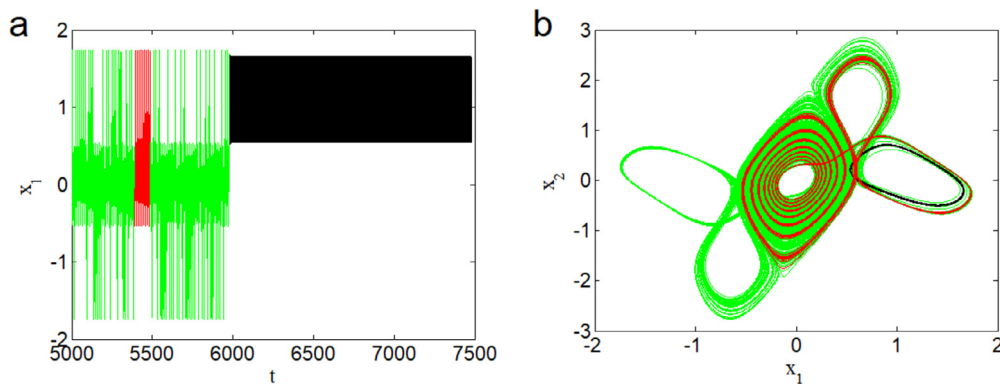
Fig. 9. Time series and phase portrait illustrating the intermittence chaos (chaotic attractor in green, and limit cycle periodic-10 and 7 red and black color respectability) observed in this model for $w_{22} = 0.387$ and initial conditions $(0, 1, 0.1)$.

$$\begin{cases} \dot{x}_1 = -x_1 + w_{11}f_1(x_1) + w_{12}f_2(x_2) + \beta w \\ \dot{x}_2 = -x_2 + k(\phi^2 - 0.5)f_1(x_1) + w_{22}f_2(x_2) \\ \dot{\phi} = f_1(x_1) - 2\phi \\ \dot{w} = -\varepsilon w - \beta(\phi - \gamma) \end{cases} \tag{7}$$

Bifurcation diagram displaying in Fig. 11(a1)-(a2) the control of multiple periodic state to a monostable state of strange attractors wish represent the normal state in the brain. Where we can clearly see the evolution of multistable states to the monostable state. When $0 \leq \beta \leq 0.0016$, the model conserve a multistable state of four periodic attractors. We can observe the coexistence of two attractors for $0.000162 \leq \beta \leq 0.0176$. In the area $0.0178 \leq \beta \leq 0.038$, the control of multistate present monostable of periodic attractor. When $\beta = 0.04$ the model present a normal state of brain (as shown in Fig. 11 (b1)-(b2)). With parameter set and $w_{11} = -0.97$, $w_{12} = 1.25$, $k = 10$, $\varepsilon = 0.005$ and $\gamma = 0.01$.

5. Experimental investigations

Microcontrollers based implementation offer great flexibility and make it easy to implement complex systems [4]. Two Arduino boards are used for experimental validation issue. ATMEGA2560 microcontroller with the corresponding continuous time equations are discretized based on the fourth-order Runge-Kutta numerical method. The digital bits are converted into analog voltages by using two R-2R resistors ladders of 16-bit [10]. Arduino Uno microcontroller is use to return the output analog signal on a computer for data acquisition and representation as shown in Fig. 12 with corresponding photograph of experimental set-up. We present in Fig. 12 a microcontroller based implementation of

a four-scroll attractor in the plane (x_1, x_2) for $w_{11} = -0.97$, $w_{12} = 1.25$, $k = 10$, $w_{22} = -0.073$ and initial conditions $(0, 0, 0)$. The phase portraits of Fig. 12 (a1)-(a2) correspond to the numerical analysis provided in Fig. 5 (d1). We also show multistability of two and four different attractors obtained for $w_{22} = -0.376$, and $w_{22} = -0.381$ presented in Fig. 13 (a1)-(a2) and Fig. 14 (a1-a4) respectively with parameter set $w_{11} = -0.97$, $w_{12} = 1.25$, and $k = 10$. Those results coexistence correspond with numerical simulation present in Fig. 6 (b1-c2). It appears that microcontroller based implementation results are in agreement with those of the numerical analysis.

6. Conclusion

In this paper, we have investigated the complex dynamic behaviors of an HNN based on bi-neuron with a memristive synaptic weight. By considering the flux controlled memristor recently proposed in literature [20] where the authors provided double-scroll attractors and coexistence of three attractors. Studies intermittence bifurcation of the dynamic behaviors of the system exhibits up to four different attractors coexisting in the new model. Various four-scroll attractors is also report in this paper. Furthermore, transient chaos, intermittence chaos and the presence of bursting oscillations are emerged in this neural network. To obtain the normal state of the brain, control of periodic oscillations is well done. Microcontroller based implementation are used to confirm numerical analysis. To the best of author's knowledge, this works present a simple configuration of four-scroll attractor with only two neurons. The application part of this work, as well as the encryption process, represents the topic of our future work. Moreover, the
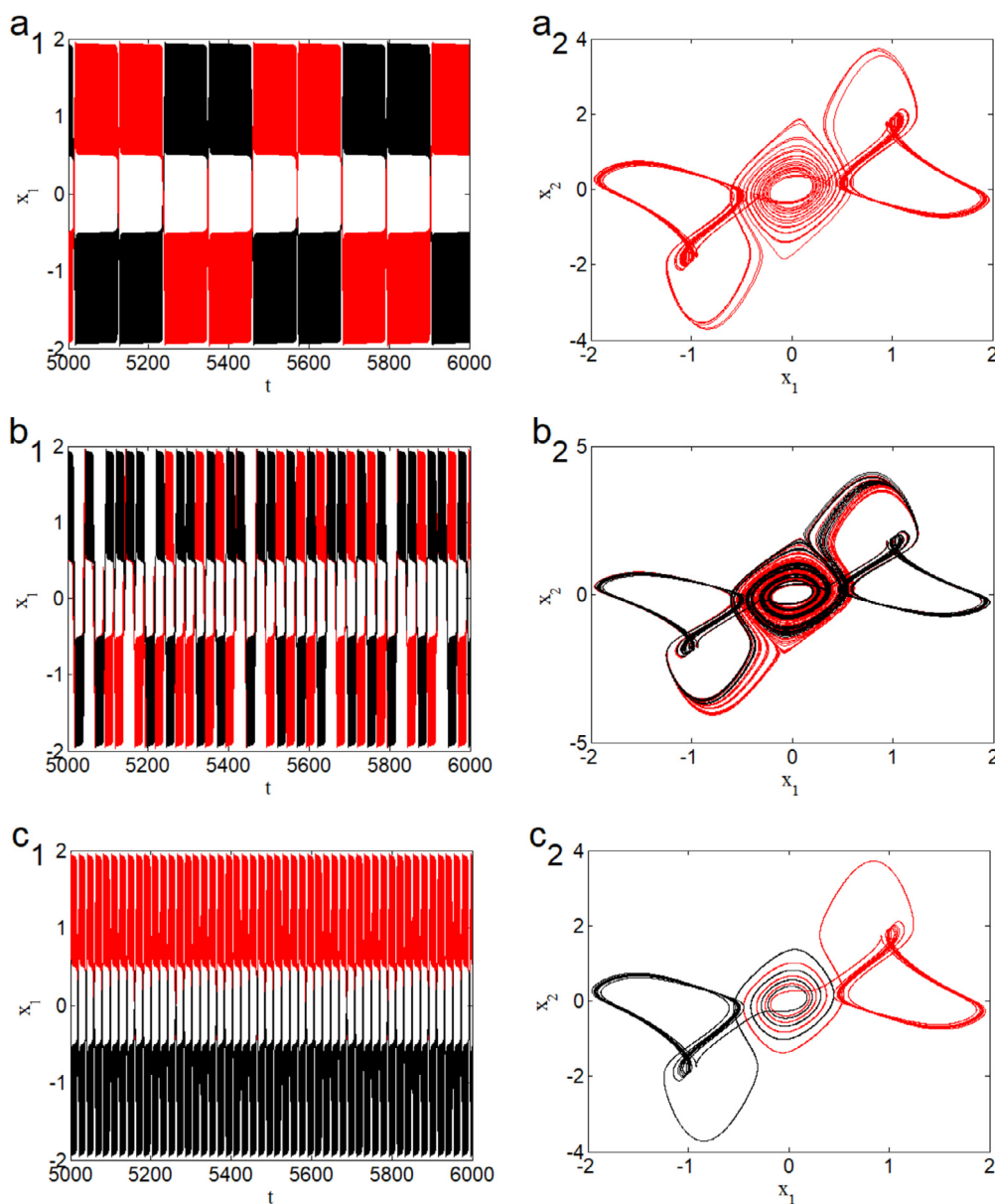
Fig. 10. Regular to irregular behavior of bursting oscillations when the value of synaptic weight w_{22} is increase. (a)-(c) regular bursting oscillations when $w_{22} = 0.278$, $w_{22} = 0.29$ and irregular bursting oscillations for $w_{22} = 0.285$ (b).

experimental implementation of the control strategy is interesting and deserves further studies.

Declarations

Author contribution statement

Bertrand Frederick Boui A Boya, Mr: Conceived and designed the experiments; Performed the experiments; Analyzed and interpreted the data; Contributed reagents, materials, analysis tools or data; Wrote the paper.

Jacques Kengne, Professor: Conceived and designed the experiments; Analyzed and interpreted the data; Contributed reagents, materials, analysis tools or data; Wrote the paper.

Germaine Djuidje Kenmoe, Professor; Joseph Yves Effa, Professor: Conceived and designed the experiments; Analyzed and interpreted the data; Contributed reagents, materials, analysis tools or data.

Data availability statement

No data was used for the research described in the article.
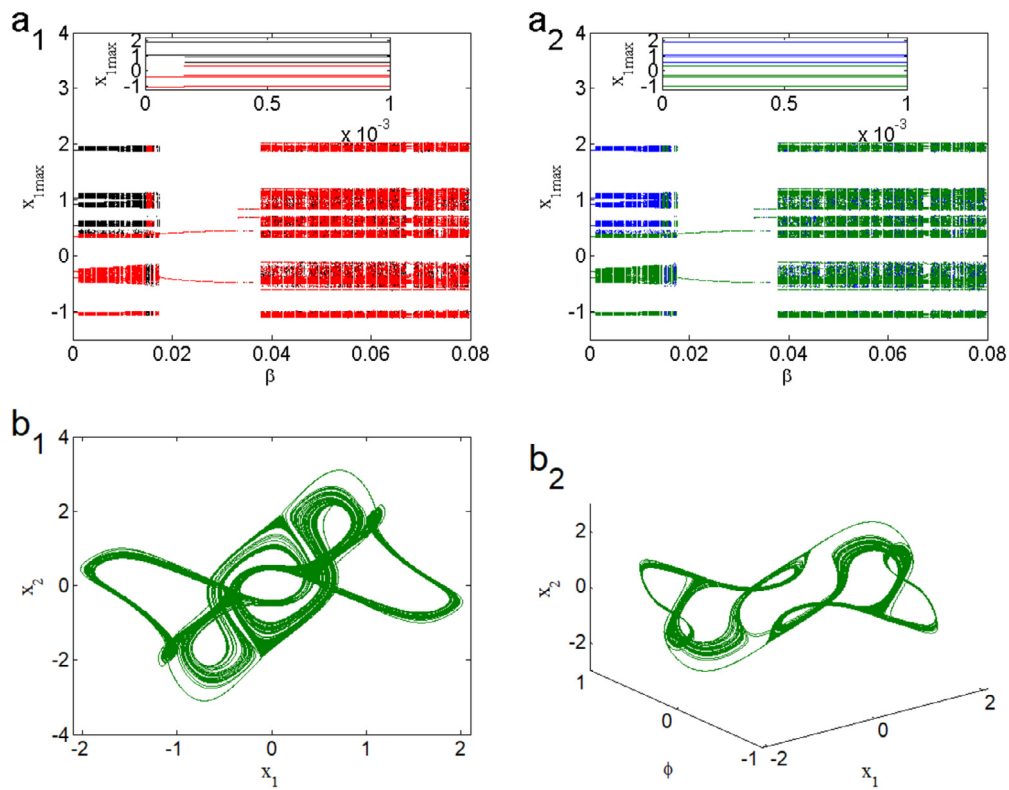
Declaration of interest's statement
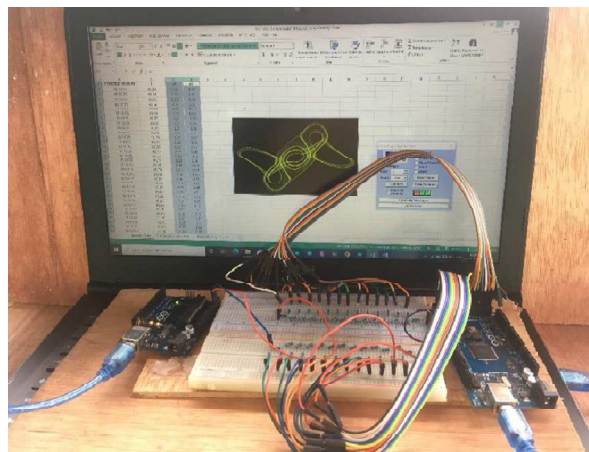
The authors declare no conflict of interest.

Additional information

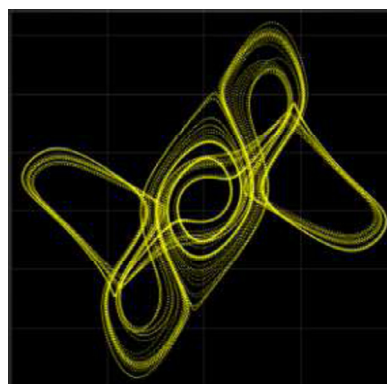No additional information is available for this paper.

Fig. 11. (a) Bifurcation diagrams illustrating the control of multistability to monostability when increase the coupling strength of control β. Projection of the monostable state in (x_1, x_2) and (b) the strange attractors in space (x_1, ϕ, x_2).
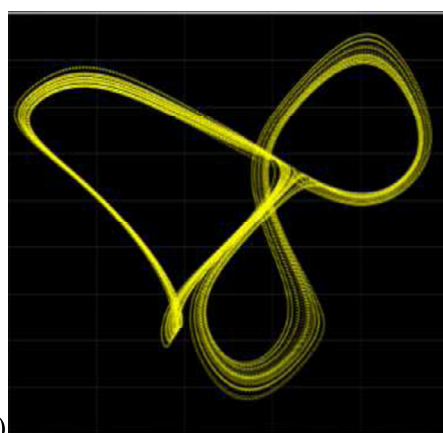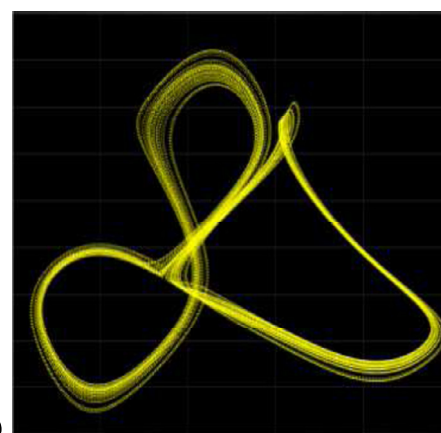
(a1)

(a2)

Fig. 12. (a1) The photograph of the experimental set-up, displaying chaotic four-scroll attractor observed from the microcontroller based implementation of system (3) in the plane (x_1, x_2) for $w_{22} = -0.073$. (a2) Zoom of Fig. 12 (a1).

(a1)

(a2)

Fig. 13. Experimental validation with microcontroller based implementation showing coexistence of two different strange two-scroll attractors observed when $w_{22} = -0.376$ in the plane (x_1, x_2).
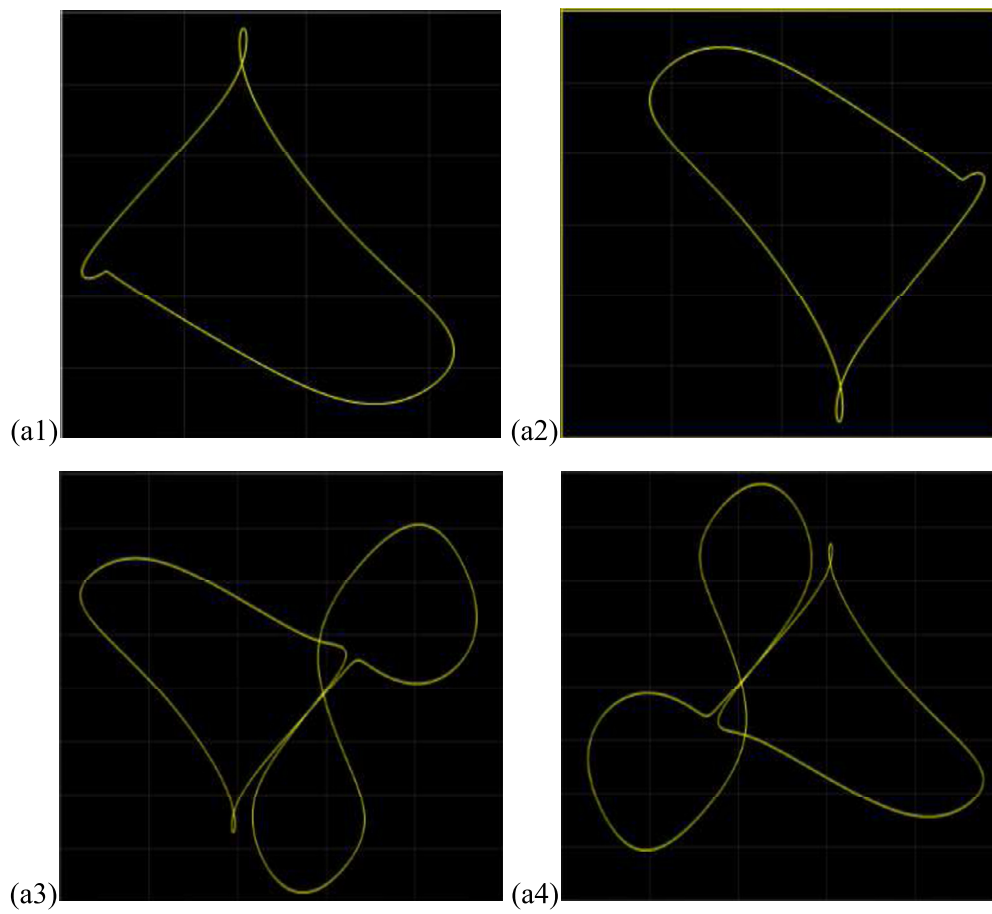
Fig. 14. Experimental validation with microcontroller implementation showing coexistence of four different periodic state for $w_{22} = -0.381$ in the plane (x_1, x_2).

References

[1] J.J. Hopfield, Neural networks and physical systems with emergent collective computational abilities, Proc. Natl. Acad. Sci. 79 (1982) 2554–2558.

[2] I.S. Doubla, B. Ramakrishnan, Z.N. Tabekoueng, J. Kengne, K. Rajagopal, Infinitely many coexisting hidden attractors in a new hyperbolic-type memristor-based HNN, Eur. Phys. J. Spec. Top. (2022) 1–15.

[3] K. Rajagopal, J.M. Munoz-Pacheco, V-T. Pham, D.V. Hoang, F.E. Alsaadi, F.E. Alsaadi, A Hopfield neural network with multiple attractors and its FPGA design, Eur. Phys. J. Spec. Top. 227 (2018) 811–820.

[4] Q. Lai, C. Lai, P.D.K. Kuate, C. Li, S. He, Chaos in a simplest cyclic memristive neural network, Int. J. Bifurc. Chaos 32 (2022) 2250042.

[5] Q. Li, S. Tang, H. Zeng, T. Zhou, On hyperchaos in a small memristive neural network, Nonlinear Dyn. 78 (2014) 1087–1099.

[6] V-T. Pham, C. Volos, S. Jafari, X. Wang, S. Vaidyanathan, Hidden hyperchaotic attractor in a novel simple memristive neural network, Optoelectron. Adv. Mater., Rapid Commun. 8 (2014) 1157–1163.

[7] F. Yu, H. Chen, X. Kong, Q. Yu, S. Cai, Y. Huang, et al., Dynamic analysis and application in medical digital image watermarking of a new multi-scroll neural network with quartic nonlinear memristor, Eur. Phys. J. Plus 137 (2022) 1–14.

[8] F. Yu, H. Shen, Z. Zhang, Y. Huang, S. Cai, S. Du, Dynamics analysis, hardware implementation and engineering applications of novel multi-style attractors in a neural network under electromagnetic radiation, Chaos Solitons Fractals 152 (2021) 111350.

[9] S. Doubla Isaac, Z.T. Njitacke, J. Kengne, Effects of low and high neuron activation gradients on the dynamics of a simple 3D hopfield neural network, Int. J. Bifurc. Chaos 30 (2020) 2050159.

[10] B.F.B.A. Boya, B. Ramakrishnan, J.Y. Effa, J. Kengne, K. Rajagopal, The effects of symmetry breaking on the dynamics of an inertial neural system with a non-monotonic activation function: theoretical study, asymmetric multistability and experimental investigation, Phys. A, Stat. Mech. Appl. (2022) 127458.

[11] F. Wu, Y. Guo, J. Ma, Reproduce the biophysical function of chemical synapse by using a memristive synapse, Nonlinear Dyn. (2022) 1–22.

[12] H. Bao, W. Liu, Aihuang Hu, Coexisting multiple firing patterns in two adjacent neurons coupled by memristive electromagnetic induction, Nonlinear Dyn. (2019).

[13] H. Lin, C. Wang, Influences of electromagnetic radiation distribution on chaotic dynamics of a neural network, Appl. Math. Comput. 369 (2020) 124840.

[14] F. Wu, X. Hu, J. Ma, Estimation of the effect of magnetic field on a memristive neuron, Appl. Math. Comput. 432 (2022) 127366.

[15] H. Lin, C. Wang, W. Yao, Y. Tan, Chaotic dynamics in a neural network with different types of external stimuli, Commun. Nonlinear Sci. Numer. Simul. 90 (2020) 105390.

[16] Q. Xu, Z. Song, H. Bao, M. Chen, B. Bao, Two-neuron-based non-autonomous memristive Hopfield neural network: numerical analyses and hardware experiments, AEÜ, Int. J. Electron. Commun. 96 (2018) 66–74.

[17] X-S. Yang, Q. Yuan, Chaos and transient chaos in simple Hopfield neural networks, Neurocomputing 69 (2005) 232–241.

[18] C. Chen, J. Chen, H. Bao, M. Chen, B. Bao, Coexisting multi-stable patterns in memristor synapse-coupled Hopfield neural network with two neurons, Nonlinear Dyn. 95 (2019) 3385–3399.

[19] C. Chen, H. Bao, M. Chen, Q. Xu, B. Bao, Non-ideal memristor synapse-coupled bi-neuron Hopfield neural network: numerical simulations and breadboard experiments, AEÜ, Int. J. Electron. Commun. 111 (2019) 152894.

[20] M. Hua, H. Bao, H. Wu, Q. Xu, B. Bao, A single neuron model with memristive synaptic weight, Chin. J. Phys. 76 (2022) 217–227.

[21] Y.Q. Fei, Huifeng Yu, Xinxin Chen, Abdulmajeed Kong, Dynamic analysis and audio encryption application in IoT of a multi-scroll fractional-order memristive Hopfield neural network, Fractal Fract. (2022).

[22] Ali H. Nayfeh, Balakumar Balachandran, Applied Nonlinear Dynamics: Analytical, Computational and Experimental Methods, Wiley, 1995.

[23] A.N. Pisarchik, A.E. Hramov, Emergence of Multistability. Multistability in Physical and Living Systems, Springer, 2022, pp. 45–110.

[24] J.P. Newman, R.J. Butera, Mechanism, dynamics, and biological existence of multistability in a large class of bursting neurons, Chaos 20 (2) (2010) 023118.

[25] D. Angeli, J.E. Ferrell Jr., E.D. Sontag, Detection of multistability, bifurcations, and hysteresis in a large class of biological positive-feedback systems, Proc. Natl. Acad. Sci. USA 101 (7) (2004) 1822–1827.

[26] M.K.N. Laurent, Multistability: a major means of differentiation and evolution in biological systems, Trends Biochem. Sci. 24 (1999) 418–422.

[27] S. Panahi, Z. Aram, S. Jafari, J. Ma, J. Sprott, Modeling of epilepsy based on chaotic artificial neural network, Chaos Solitons Fractals 105 (2017) 150–156.

[28] J.T. Fossi, H.C. Edima, Z.T. Njitacke, F.F. Kemwoue, J.M. Mendimi, J. Atangana, Coexistence of attractors and its control with selection of a desired attractor in a model of extended Hindmarsh–Rose neuron with nonlinear smooth fitting function: microcontroller implementation, J. Vibr. Eng. Technol. (2022) 1–14.

[29] H. Lin, C. Wang, Y. Tan, Hidden extreme multistability with hyperchaos and transient chaos in a Hopfield neural network affected by electromagnetic radiation, Nonlinear Dyn. 99 (2020) 2369–2386.

[30] Fu-Ping Wang, Fa-Qiang Wang, Multistability and coexisting transient chaos in a simple memcapacitive system, Chin. Phys. B 29 (5) (2020) 058502.

[31] Y.V. Bakhanova, A.O. Kazakov, A.G. Korotkov, T.A. Levanova, G.V. Osipov, Spiral attractors as the root of a new type of "bursting activity" in the Rosenzweig–MacArthur model, Eur. Phys. J. Spec. Top. 227 (2018) 959–970.

[32] Z.T. Njitacke, J. Awrejcewicz, A.N.K. Telem, T.F. Fozin, J. Kengne, Complex dynamics of coupled neurons through a memristive synapse: extreme multistability and its control with selection of the desired state, IEEE Trans. Circuits Syst. II, Express Briefs (2022).

[33] Z.T. Njitacke, S.D. Isaac, T. Nestor, J. Kengne, Window of multistability and its control in a simple 3D Hopfield neural network: application to biomedical image encryption, Neural Comput. Appl. 33 (2021) 6733–6752.

[34] P. Sharma, M. Shrimali, A. Prasad, N. Kuznetsov, G. Leonov, Control of multistability in hidden attractors, Eur. Phys. J. Spec. Top. 224 (2015) 1485–1491.